

Analyst

Accepted Manuscript

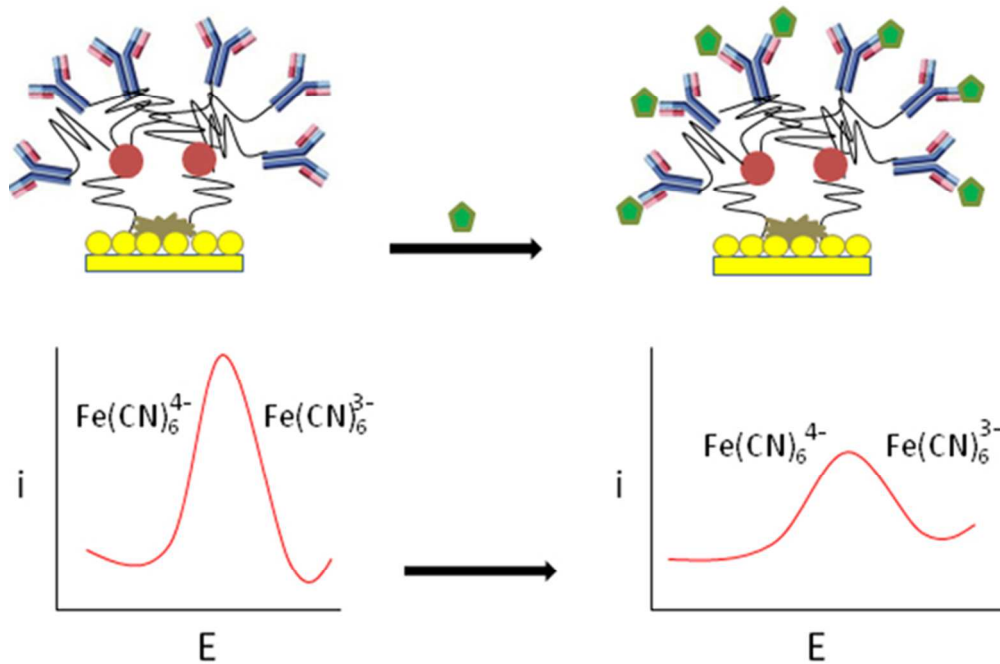


This is an *Accepted Manuscript*, which has been through the Royal Society of Chemistry peer review process and has been accepted for publication.

Accepted Manuscripts are published online shortly after acceptance, before technical editing, formatting and proof reading. Using this free service, authors can make their results available to the community, in citable form, before we publish the edited article. We will replace this *Accepted Manuscript* with the edited and formatted *Advance Article* as soon as it is available.

You can find more information about *Accepted Manuscripts* in the [Information for Authors](#).

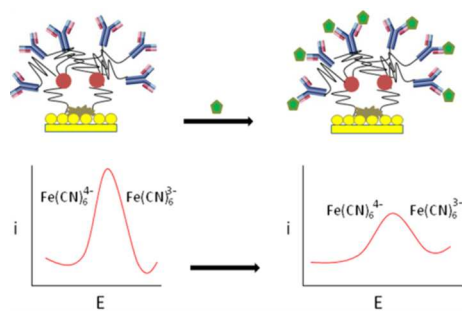
Please note that technical editing may introduce minor changes to the text and/or graphics, which may alter content. The journal's standard [Terms & Conditions](#) and the [Ethical guidelines](#) still apply. In no event shall the Royal Society of Chemistry be held responsible for any errors or omissions in this *Accepted Manuscript* or any consequences arising from the use of any information it contains.



Graphical Abstract
60x39mm (300 x 300 DPI)

1
2
3
4
5
6
7
8
9
10
11
12
13
14
15
16
17
18
19
20
21
22
23
24
25
26
27
28
29
30
31
32
33
34
35
36
37
38
39
40
41
42
43
44
45
46
47
48
49
50
51
52
53
54
55
56
57
58
59
60

1
2
3
4
5
6 This paper presents a facile and highly sensitive label free electrochemical
7
8 immunosensor for breast cancer biomarker using antiHER2- Fe₃O₄ NP
9
10 bioconjugate.
11



1
2
3 Electrochemical immunosensor for breast cancer biomarker based on antiHER2-Iron oxide
4
5 Nanoparticle Bioconjugate
6
7
8
9

10
11 Mahdi Emami^a, Mojtaba Shamsipour^b, Reza Saber^{c,d,*}, Rasoul Irajirad^d
12
13
14
15
16

17 ^aSchool of chemistry, University college of science, University of Tehran, Tehran, Iran
18
19

20 ^bDepartment of chemistry, Razi university, Kermanshah, Iran
21
22

23 ^cDepartment of nanotechnology, School of Advanced Technologies in Medicine, Tehran university of
24 medical science, Tehran, Iran
25
26
27

28 ^dResearch center for science and technology in medicine, Imam Khomeini hospital, Tehran, Iran
29
30
31
32
33

34
35 *Corresponding Author. Tel. +98 21 66907525 fax: +98 21 66581533.
36
37

38 E-mail address: rsaber92@yahoo.com (R. Saber).
39
40
41
42
43
44
45
46
47
48
49
50
51
52
53
54
55
56
57
58
59
60

Abstract

A label free immunosensor was designed for ultra detection of human epidermal growth factor receptor 2 (HER2) in real samples using differential pulse voltammetry (DPV) method. In a separate process, antiHER2 antibodies were attached to iron oxide nanoparticles (FeNPs) to form stable bioconjugates which were later laid over the gold electrode surface. In this way, by the advantage of their long terminals, the bioconjugates provided the most possible space for the immunoreaction between biomolecules. Under optimal conditions, the immunosensor was responsive to HER2 concentrations over the ranges of $0.0 \text{--} 10 \text{ ng mL}^{-1}$ and $10 \text{--} 100 \text{ ng mL}^{-1}$ linearly and benefited from a satisfying detection limit as low as 0.995 pg mL^{-1} and a favorable sensitivity as sharp $5.921 \cdot \text{A mL ng}^{-1}$. The reliability of the method in clinical analysis was proved by successful quantization of HER2 levels in serum samples obtained from patients. Furthermore, the precision and the stability of the method were evaluated and verified to be acceptable in immunoassay studies.

Keywords: Electrochemical immunosensor, HER2, bioconjugate breast cancer gold electrode

1. Introduction

To realize low-level of tumor biomarkers is vital for early awareness of cancer and commence the appropriate treatment processes. Human epidermal growth factor receptor 2 (HER2) as a key prognostic marker [1], is over-expressed in 10-25% of breast cancer [2] which is one of the most common malignant type of tumor in women [3]. To establish a fast technique sensitive to the low-levels of HER2 biomarker which result in early diagnosis of the cancer is of great significance not only for increasing the survival rate but also for saving cost and time in successful prognosis of the disease.

For this purpose, several techniques [4-7] were developed focusing on detection of HER2 positive cells which are usually taken out in invasive methods like biopsy and are not available in human serum. In comparison to these techniques, electrochemical techniques by the use of bioconjugate modified electrodes are the most desired systems owing their excellent sensitivity, rapidity, low cost and easy

operation. Typically there are two kinds of electrochemical detection platforms for biomarker proteins. The first kind is labeled method known as sandwich type method in which an enzyme, usually horseradish peroxidase, is attached to a secondary antibody (Ab). This labeled Ab remains tied to the biomarker attached to the primary Ab and usually catalyzes the reduction of hydrogen peroxide to represent a measurable signal [8, 9]. However, other nanomaterials such as CdS and silver nanoparticles can also be attached to secondary antibodies and their stripping signals corresponding to the concentration of biomarkers be recorded subsequently [10, 11]. Although this strategy is assumed as a highly sensitive method, but problems such as sample pretreatment, separation and purification process of secondary Ab limit the approach. In the second kind, known as label free method, decrease in signal intensity of a redox probe is directly related to the concentration of biomarker, which is bound to a modified surface and hinder the electron transfer processes [12, 13]. Eliminating time-consuming extra processes makes this method more simple, quick and desired.

Lately, functionalized nanoparticles specially functionalized iron oxide nanoparticles (Fe_3O_4 NPs) have attracted much attention in the fabrication of biosensing systems due to their unique properties such as biocompatibility, signal amplification and their ability to bind covalently to Abs via their functional groups [14, 15].

The extensive use of poly ethylene glycol (PEG), as a long compatible linker for nanoparticles, has been treated well [16-18]. The main advantage of using PEG is to provide enough space to bind more Abs to nanoparticles and allow them to stand aside and result more effective combination with the targets.

In this work, we attached different proportions of anti-HER2 Ab to the pegylated Fe_3O_4 NPs to form highly loaded bioconjugate. Designing a label free platform, the most appropriate bioconjugate was stabilized covalently on the surface of gold electrode to assay ultra-low level of HER2 antigen in serum samples. This highly sensitive and simple electrochemical analysis method has great potential for detection of all other biomarkers in clinical diagnostics.

2. Experimental

2.1. Apparatus and conditions

CV and DPV measurements were conducted on a μ Autolab Type III Potentiostat/Galvanostat. A three electrode cell system was used for the electrochemical experiments. Modified gold electrode was used as the working electrode. Platinum wire and Ag/AgCl (Saturated KCl) electrode were used as the counter electrode and the reference electrode, respectively. The EIS spectra were recorded with an Autolab Eco Chemie. B.V. Potentiostat/Galvanostat using the same electrode system.

The transmission electron microscopy (TEM) images were obtained from a TEM 208 Philips at an acceleration voltage of 100 kV. TIR spectra were recorded with Bruker vertex 70v. The surface morphologies of GE and GNPs/GE were evaluated by field effect scanning electron microscopy (FESEM) at an accelerating voltage of 20 kV.

2.2. Materials and reagents

AntiHER2Ab (Herceptin, 150 mg) was purchased from F. Hoffmann Roche Ltd (Switzerland). Active HER2, 5 μ g, was obtained from Biovision Inc. (USA). Poly (ethylene glycol) - maleimide - NHS ester (Mal- PEG-NHS, MW, 2000) was purchased from MANOCS (USA). Bovine serum albumin (BSA), N-hydroxy succinimide (NHS), ethyl-3-(3-dimethylaminopropyl) carbodiimide (EDC), cysteamine (Cys), 2-iminithiolane (Trautman's reagent), gold (III) chloride hydrate, sodium phosphate dibasic, potassium phosphate monobasic and 3-mercaptopropionic acid (MPA) were purchased from Sigma Aldrich Ltd (USA). Iron (III) chloride hexahydrate, iron (II) chloride tetra hydrate, hydrochloric acid (37%), methanol, toluene, 3-aminopropyltrimethoxysilane (APTMS) and ammonium hydroxide (32%) were purchased from Merck (Germany). Phosphate buffered solutions (PBS) were prepared using 0.1M Na_2HPO_4 and 0.1M KH_2PO_4 . All other chemicals and reagents were of analytical grade and were prepared using redistilled water.

2.3. Production of functionalized Fe₃O₄ NPs

2.3.1. Synthesis of bare Fe₃O₄ NPs

Fe₃O₄ NPs were synthesized based on the most common method [19]. Briefly, FeCl₂·4H₂O (0.397 g in 1 mL of 2 M hydrochloric acid) was added to FeCl₃·6H₂O (1.08 g in 4 mL of 2 M hydrochloric acid) under strong stirring over a magnetic stirrer. Then 50 mL of 0.7 M ammonium hydroxide was added to the mixture drop wisely. At the end of the reaction, the black suspension of iron oxide was separated by a permanent magnet and then redispersed in 10 mL of methanol.

2.3.2. Synthesis of the amino-Fe₃O₄ NPs (APTMS-coated Fe₃O₄ NPs)

Bare Fe₃O₄ NPs tend to aggregate and therefore it is better to start the modification process of the surface immediately. 35 mL of toluene and 25 μL of APTMS were added to 0.1 g of bare Fe₃O₄ NPs. The mixture was sonicated in a bath sonicator for 30 min. Afterwards, the mixture was heated in an oven at 60 °C for 7 h. Finally, the obtained APTMS-coated Fe₃O₄ NPs was separated by permanent magnet and redispersed in 50 mL of methanol.

2.3.3. Synthesis of PEG-amine-coated Fe₃O₄ NPs

The resulted nanoparticles were introduced with NHS-PEG2000Mal to obtain sulfhydryl reactive pegylated nanoparticles through activation of the surface amine groups. For this purpose, 31 mg of NHS-PEG2000Mal was added to 10 mL of redistilled water containing 10 mg of nanoparticles. After sonication for 30 min the mixture was stirred vigorously for 12 h. Finally, pegylated nanoparticles were separated by magnet and redispersed in 5 mL of redistilled water.

2.4. Preparation of the bioconjugates

The bioconjugates were prepared based on a reported method [20] with some modifications. Scheme 1 shows the bioconjugate preparation procedure.

1
2
3
4
5
6
7
8
9
10
11
12
13
14
15
16
17
18
19
20
21
22
23
24
25
26
27
28
29
30
31
32
33
34
35
36
37
38
39
40
41
42
43
44
45
46
47
48
49
50
51
52
53
54
55
56
57
58
59
60

Scheme 1 Preparation of the bioconjugate

2.4.1. Thiolation of antiHER2Abs

A solution of antiHER2Ab (1 mg mL^{-1}) in 0.1 M PBS pH 8 was prepared first. For thiolation of Abs, it was followed by adding 100-fold molar excess of 2-mercaptoethanol to the prepared solution. To protect the thiol groups from oxidation, 5 mM EDTA was also added to the mixture. The mixture was left for 1 h under constant stirring at room temperature. Afterwards, thiolated Abs were purified by dialysis against 20 mL of PBS pH 8, 5 times each for 1 h.

2.4.2. Attachment of anti-HER2 Abs to the NPs

The Abs-labeled nanoparticle conjugate was prepared through the following approach: 1 mg of nanoparticles (5 mg mL^{-1}) was incubated with different aliquots (50, 100, 200, or 300 μL) of thiolated Abs (1 mg mL^{-1}) over night at room temperature under constant shaking. The thiol groups of Abs were covalently attached to the unsaturated bond of maleimide linked to the nanoparticle to form the bioconjugate. The bioconjugates, then, were separated by magnet and redispersed in 1 mL PBS pH 7.2.

2.5. Fabrication of the immunosensor and electrochemical procedure

The fabrication process of the immunosensor is represented in scheme 2. Firstly, the gold electrode (GE) surface ($\pi = 3 \text{ mm}$) was polished with 0.1 μm alumina slurry on a polishing cloth for 1 min and was then ultrasonically cleaned with ethanol and redistilled water each for 3 min respectively. Afterward, the electrode was immersed in piranha solution ($\text{H}_2\text{SO}_4 : \text{H}_2\text{O}_2$, 3:1) for 5 min and then washed with pure water several times. The gold nanoparticles (GNPs) were electrodeposited on the cleaned electrode surface from solution containing 0.06 mM HAuCl₄ and 0.1 M KCl by cycling potential between 0.5 and -0.5 V for 20 times with the scan rate of 0.2 V s^{-1} . The gold modified electrode was immersed in 0.1 M MPA for 12 h at room temperature to form MPA/GNPs/GE. The resulting electrode was rinsed with redistilled water to remove physically adsorbed materials. Thereafter, 30 μL of solution containing 0.1 M EDC + 0.1 M NHS was dropped and maintained onto the surface for 2 h at room temperature to activate the carboxyl groups. After being washed with pure water, the electrode was immersed into 0.1 M Cys Solution for 8 h at room temperature to form Cys/MPA/GNPs/GE via amide formation. Subsequently, after being rinsed with redistilled water, to prepare Bioconjugate/Cys/MPA/GNPs/GE, the obtained electrode was introduced to 30 μL of bioconjugate and left for 8 h in 4 °C. The double bond in free maleimides of bioconjugate readily reacts with thiol groups from Cys to form a stable carbon-sulfur bond [21]. Excessive and physically adsorbed bioconjugates were washed away with PBS (pH 7.2) and redistilled water respectively. The process was followed by casting 20 μL of BSA (1 mg mL^{-1}) over the electrode and keeping for 45 min at 37 °C to block any possible nonspecific binding sites. Finally

1
2
3 BSA/Bioconjugate/Cys/MPA/GNPs/GE was rinsed with PBS (0.1 M, pH 7.2) and redistilled w
4 respectively. The resulting electrode was then incubated with 20 μ L different concentrations of HER
5 antigen for 30 min at 37 °C and was washed again with PBS (0.1 M, pH 7.2) and redistilled water
6 respectively. Finally, DVPs of the redox probe solution (PBS 0.05 M, pH 7.2 containing 5 mM of
7 $\text{Fe}(\text{CN})_6^{3-/4-}$) were recorded from -0.2 to 0.5 V using HER2/BSA/Bioconjugate/Cys/MPA/GNPs/GE.
8
9
10
11
12
13
14
15
16
17
18
19
20
21
22
23
24
25
26
27
28
29
30
31
32
33
34
35
36
37
38
39
40
41
42
43
44
45
46

47 Scheme 2. Graphical illustration of the construction procedure of the immunosensor and HER2 detection.
48

49 2.6. Patient serum analysis

50
51
52

53 Fresh serum samples, collected from patients in different stages of the cancer, were obtained kindly from
54 the central clinical laboratory of Imam Reza hospital, Kermanshah, Iran. Serum samples were diluted
55 with PBS (0.1M, pH 7.2) for 20 times and then 20 μ L of the samples was dropped onto the prepared
56
57
58
59
60

1
2
3 electrode and kept for 30 min at 37 °C. Finally, DPVs of the probe solution were recorded after rinsing
4 the electrode with PBS and distilled water respectively. HER2 levels for three replicates were calculated
5 using calibration regression equations.
6
7
8

9 10 2.7. Recovery test

11
12 Fresh serum samples of two healthy females were obtained from Imam Khomeini hospital. After 20 times
13 dilution with PBS (0.1M, pH 7.2), serum samples were spiked with two different concentrations of
14 HER2. The spiked concentrations were assayed using standard addition method.
15
16
17
18
19

20 21 2.8. Electrochemical measurements

22
23 Cyclic voltammograms (CVs) were recorded between 0.2 and 0.5 V with the scan rate of 20 mV/s
24 0.1 M PBS pH 7.2 containing 10 mM $\text{Fe}(\text{CN})_6^{4-}$. The parameters for DPVs, taken from the same probe
25 solution, were: pulse width of 0.06 s, pulse increment of 5 mV, pulse period of 0.1 s, pulse amplitude of
26 55 mV and scan rate of 50 mV/s.
27
28
29
30
31
32

33 EIS measurements were conducted for 0.1 M PBS pH 7.2 containing 2 mM $\text{Fe}(\text{CN})_6^{4-}$ in a frequency
34 range from 0.1 to 100 kHz. The amplitude of the applied sine wave was 10 mV with the direct current
35 potential set at 0.2 V.
36
37
38
39

40 41 3. Results and discussion

42 43 3.1. Characterization of Fe_3O_4 NPs

44
45 The morphology and size distribution of Fe_3O_4 NPs was characterized by TEM. As can be observed in
46 Fig.1A, spherical nanoparticles with the average size of about 20 nm were distributed uniformly. SEM
47 was also used to confirm the electrodeposition process. Figs.1B and C exhibit the surface of the electrode
48 before and after electrodeposition of the nanoparticles, respectively. A rough and stone surface is
49 obtained in consequence of gold electrodeposition.
50
51
52
53
54
55
56
57
58
59
60

1
2
3
4
5
6
7
8
9
10
11
12
13
14
15
16
17
18
19
20
21
22
23
24
25
26
27
28
29
30
31
32
33
34
35
36
37
38
39
40
41
42
43
44
45
46
47
48
49
50
51
52
53
54
55
56
57
58
59
60

Fig. 1. (A) TEM image of Fe_3O_4 NPs, (B and C) FESEM images of gold electrode surface before and after GNPs electrodeposition, respectively (D) IR spectra of APTMS-coated Fe_3O_4 NPs (E) CVs of 0.1 M PBS pH 7.2 containing 10 mM $\text{Fe}(\text{CN})_6^{3-/4-}$ at a: MPA/GNPs/GE and b: Fe_3O_4 NPs/ MPA/GNPs/GE

FT-IR spectroscopy was operated to validate the presence of APTMS at the surface of APTMS-coated Fe_3O_4 NPs. The spectrum in Fig. 1D shows a sharp band around 530 cm^{-1} for iron oxide NPs and three moderate bands at 1100, 1620 and 2930 cm^{-1} that can be assigned to vibration of Si-N-H and stretching of C-H, respectively.

To characterize the APTMS-coated Fe_3O_4 NPs electrochemically, MPA/GNPs/GE was modified with the nanoparticles through combining carboxyl and amine groups and its performance was observed before and after modification using CV technique. As can be seen in Fig. 1E, the presence of the NPs intensifies the redox signal distinctly. As an explanation for this event, the intrinsic properties of nano-sized iron oxide particles decorated with functional groups facilitate the electron transfer (ET) process between the probe and the electrode. This desirable quality of the functionalized Fe_3O_4 NPs makes them proper candidates for Ab to be loaded over and to form bioconjugates for using in electrochemical systems.

3.2. Characterization of the immunosensor

The most common technique CV was initially used to monitor each step of modification of the gold electrode surface (Fig. 2A, B). As can be seen, a pair of redox peaks is observed for 10 mM of $\text{Fe}(\text{CN})_6^{3-/4-}$ in PBS (0.1 M, pH 7.2) at bare gold electrode ($E_p = 94$ mV). Sharper redox peaks with less difference in peak potential ($\Delta E = 76$ mV) were noticed for the electrode after electrodeposition of gold nanoparticles (b). Subsequently, at the end of immersion of GNPs/GE in MPA solution to obtain MPA/GNPs/GE through formation of Au-S bonds, redox peaks increased again clearly (c). In here, dangling carboxyl groups at the surface may facilitate the electron transfer (ET) process between the probe and the electrode. Further modification of the electrode with Cys reduced the redox peaks (d). It is probably due to the ET blockage in consequence of increasing the length of carbon chain as well as

1
2
3 turning carboxyl groups to terminal sulfhydryl groups. Afterward, although Fe_3O_4 NPs because of their
4 intrinsic properties, intensify the redox signal which has been investigated in section 3, but placing of
5 the bioconjugates at the surface reduced the redox peaks since more interruption in ET process happens
6 by the presence of the huge biomolecules (Abs) on the nanoparticles. Thereafter, in order to block the
7 possible nonspecific bonding sites at Bioconjugate/Cys/MPA/GNPs/GE, BSA was applied to the surface
8 of the electrode and thus an obvious decrease in redox peaks occurred in (f). Finally, introducing of
9 HER2 (10 ng mL^{-1}) to the resulted electrode made more decrease in redox peaks.

10
11 Furthermore, electrochemical impedance spectra (EIS, Nyquist plots) were also conducted to monitor the
12 performance of the immunosensor through construction (Fig. 2C). Semicircle part of the Nyquist plots at
13 higher frequencies is related to the ET limited process, it is possible to investigate the surface change at
14 each step of the modification process by measuring the semicircle diameter which equals the ET
15 resistance (R). Spectrum (a) shows a tiny semicircle for bare gold electrode. Modification of the
16 electrode with GNPs and MPA gave smaller and quite smaller values of faradic impedance for GNPs/GE
17 and MPA/GNPs/GE respectively (b, c) indicating that these modifications increase the ET process of the
18 system. After modification of the resulted electrode with Cys, semicircle diameter was extended and
19 thus an initiated impedance was observed in (d). Predictably, after loading of the surface with
20 bioconjugates, R increased sharply because of the main hindrance against ET process caused by spacious
21 Abs (e). Comparing with other works [8, 13], in this step, less increase in R was observed that is
22 probably due to the advantageous use of iron oxide NPs with their positive effect on ET process.
23 Blocking some parts of the surface, further modification of the electrode by BSA resulted an additional
24 increase in R . (f). Finally, specific coupling of HER2 with antiHER2 Ab at the surface of the
25 immunosensor made more interference in the ET process and thus increased R in consequence (g).

1
2
3
4
5
6
7
8
9
10
11
12
13
14
15
16
17
18
19
20
21
22
23
24
25
26
27
28
29
30
31
32
33
34
35
36
37
38
39
40
41
42
43
44
45
46
47
48
49
50
51
52
53
54
55
56
57
58
59
60

Fig. 2. (A and B) CVs of 0.1 M PBS pH 7.2 containing 10 mM $\text{Fe}(\text{CN})_6^{4-}$ at a: Bare GE, b: GNPs/GE, c: MPA/GNPs/GE, d: Cys/MPA/GNPs/GE, e: Bioconjugate/Cys/MPA/GNPs/GE, f: BSA/Bioconjugate/Cys/MPA/GNPs/GE and f: HER2/BSA/Bioconjugate/Cys/MPA/GNPs/GE (C) Nyquist plots for 0.05 M PBS pH 7.2 containing 2 mM $\text{Fe}(\text{CN})_6^{4-}$ obtained at different electrodes (as A and B)

3.3. Optimization of analytical variables

3.3.1. The quantity of the stabilized Abs on the NPs

1
2
3 The effect of the amount of the Abs loaded on Fe_3O_4 NPs was investigated over the response of the
4 immunosensor. For this purpose, various loaded bioconjugates, prepared by different quantities of
5 thiolated antiHER2 (50, 100, 200 and 300 μg) were used to construct the immunosensor. As can be seen
6 in Fig. 3A, the current change is intensified by increasing the antiHER2 amount up to 200 μg . Using
7 more amount of Abs probably results in saturation of the nanoparticle surface and interference with the effective
8 binding of the bioconjugate to the surface of the electrode, so the optimum amount of antiHER2 was
9 selected to be 200 μg .

19 3.3.2. Incubation time

20 Since the formation of the covalent bonds in the modification steps is slow, the incubation time in each
21 relevant step plays an important role and needs to be optimized. Fig. 3B shows the effect of incubation
22 times of three modifier components on the immunosensor performance. The optimum incubation time
23 for MPA, Cys and antiHER2 Ab were obtained to be 12, 8 and 8 h respectively. More incubation times
24 had no positive effect on the signal most likely due to the saturation of the electrode surface

53 Fig. 3. Optimization of analytical variables. (A) Current change vs Ab amount ($n = 3$), (B) Effect of
54 incubation time over the response of the immunosensor ($n = 3$).

3.4. Analytical performance of the immunosensor

Under the most advantageous constructing conditions, the response of the immunosensor towards different concentrations of HER2 was studied by recording DPVs of PBS (pH 7.2) containing $\text{Fe}(\text{CN})_6^{3-/4-}$ with the result shown in Fig. 4A. The resulting calibration curve is linear over two concentration ranges from 0.01 to 10 ng mL^{-1} and 10 to 100 ng mL^{-1} (Fig. 4B). The correspondence calibration regression equations for lower and higher concentration ranges are $I (^A) = (5.921 \pm 0.09)[\text{HER2}] (\text{ng mL}^{-1}) + (11.507 \pm 0.11)$, $R^2 = 0.9981$ and $I (^A) = (0.300 \pm 0.008)[\text{HER2}] (\text{ng mL}^{-1}) + (69.357 \pm 0.412)$, $R^2 = 0.9913$ respectively.

Fig. 4. (A) DPVs of the probe solution taken at the immunosensor after incubation with a: 0, b: 0.01, c: 0.4, d: 1, e: 2, f: 4, g: 8, h: 10, i: 25, j: 40 and k: 100 ng mL^{-1} of HER2. (B) Calibration graph (current change vs HER2 concentrations), ($n = 4$)

The detection limit (DL) was evaluated as $\frac{3s}{m}$ and determined to be $(0.995 \pm 0.022) \text{ pg mL}^{-1}$ where s is the standard deviation of the peak current ($n = 5$) and m is the slope of the calibration curve for lower

concentration range. The sensitivity of this method (92.1 % 0.091 •A mL⁻¹) is more than five times that of the most recent method for quantification of HER2 biomarker [10]. Beside this advantage, the more convenient fabrication process and simplicity of the method would make it comparable with other methods which were reported sensitive to HER2. To corroborate the superiority of this method, a comparative study was done with the results shown in Table 1.

Table 1

Comparison of HER2 results for the recent proposed methods.

method	Linear Range (ng mL ⁻¹)	Detection limit (pg mL ⁻¹)	reference
PEMS ¹	0.05€2	25.3	22
OFRR ²	13€100	13000	23
ST-ECIS ³	6 €30	6000	24
LF-ECIS ⁴	0.01€10 10€100	0.995	This work

Piezoelectric microcantilever sensor

opto-fluidic ring resonator²

Sandwich type electrochemical immunosensor³

Label free electrochemical immunosensor⁴

3.5. Real sample analysis

The proposed method was applied to quantify HER2 concentrations in serum samples collected from several patients. Results obtained by this method were compared with those obtained by the expensive reference method enzyme-linked immunosorbent assay (ELISA) method (Table 2). From the good agreement between two methods, it can be deduced that this method can be assumed as a replacing applicable method for quantization of the biomarker.

Table 2

HER2 levels in patient serum samples obtained by the proposed and ELIZA method

Serum sample no.	Proposed method (ng mL ⁻¹), (n =3)	ELIZA method (ng mL ⁻¹)	Relative error (%)
1	13 ± 0.5	12.7 ± 0.3	2.36
2	26 ± 0.9	24.9 ± 0.1	4.41
4	24.5 ± 0.6	23.5 ± 0.3	4.25
5	61 ± 0.8	62.1 ± 0.4	-1.77
6	84.8 ± 0.9	86.1 ± 0.3	-1.51

3.6. The precision and stability study

To evaluate the precision of the method, serum samples spiked with HER2 and the recoveries were extracted using standard addition method. The percentage recoveries are for triplicates of added 2 and 20 ng mL⁻¹ HER2 were assayed to be (101 ± 0.9) % and (101.8 ± 1.2) % respectively. Satisfactory recoveries verified the good precision of the method.

The stability of the method was assessed by recording the results of the immunosensor which has been already kept in 0.1 M PBS pH 7 for three weeks at 4 °C. A (9 ± 1) % decrease in primary results indicated that the method benefits from acceptable stability (n = 3).

4. Conclusion

A facile and novel electrochemical immunosensor for detection of breast cancer biomarker was constructed based on anti-HER2₃O₄ NP bioconjugate. The use of bioconjugate not only facilitates the electron transfer in redox probe due to the good nature of the nanoparticles, it also increases the sensitivity of the method by loading as much as on the board and keeping them far enough from the electrode surface to interact with biomarkers more efficiently. The method has low detection limit with the excellent sensitivity and seems to be unique and comparable with other methods responsive to HER2

1
2
3 and could be assumed as a promising replacing technique for cancer recognition. Fe_3O_4 NPs can be
4 anchored with various Abs, so this immunoassay method holds great potential for detection of all other
5
6
7
8
9 biomarkers in clinical diagnostics.

10 11 12 13 14 15 16 17 18 19 20 21 22 23 24 25 26 27 28 29 30 31 32 33 34 35 36 37 38 39 40 41 42 43 44 45 46 47 48 49 50 51 52 53 54 55 56 57 58 59 60

References

- [1] M.A. Owens, B.C. Horter, M.M. Da Silva, HER2 amplification ratios by fluorescence in situ hybridization and correlation with immunohistochemistry in a cohort of 6556 breast cancer tissues, Clin. Breast Cancer 5 (2004) 699.
- [2] D.J. Slamon, G.M. Clark, S.G. Wong, W.J. Levin, U. Allrich, W.L. McGuire, Human breast cancer: correlation of relapse and survival with amplification of the HER-2/neu oncogene, Science, 235 (1987) 177-182.
- [3] P. Boyle, B. Levin, World Cancer Report, International Agency for Research on Cancer, 2008.
- [4] W. Lu, S.R. Arumugam, D. Senapati, A.K. Singh, T. Arbnesi, S.A. Khan, H. Yu, P.C. Ray, Multifunctional oval-shaped gold nanoparticle based selective detection of breast cancer cells using simple colorimetric and highly sensitive two-photon scattering assay, ACS Nano 4 (2010) 7139.
- [5] K. Li, R. Zhan, S.S. Feng, B. Liu, Conjugated polymer loaded nanospheres with surface functionalization for simultaneous discrimination of different cancer cells under single wavelength excitation, Anal. Chem. 83 (2011) 2132.
- [6] M.C. Tsai, T.L. Tsai, D.B. Shieh, H.T. Chiu, C.Y. Lee, Detecting HER2 on cancer cells by TiO_2 spheres Mie scattering, Anal. Chem. 81 (2009) 5996.

- 1
2
3 [7] J. Gao, K. Chen, Z. Miao, G. Ren, X. Chen, S.S. Gambhir, Z. Cheng, Affinity-based nanoprobe for
4 HER2-expressing cell and tumor imaging, *Biomaterials* 32 (2011) 2148.
5
6
7
8
9
10 [8] X. Zhua, J. Yangb, M. Liua, Y. Wua, Z. Shena, G. Li, Sensitive detection of human cancer cells
11 based on aptamer-aptamer sandwich architecture, *Anal. Chim. Acta* 764 (2013) 559.
12
13
14
15 [9] L. Wang, X. Jia, Y. Zhou, Q. Xie, S. Yao, Sandwich-type amperometric immunosensor for human
16 immunoglobulin G using antibody-adsorbed Au/SiO₂ nanoparticles, *Microchim. Acta* 168 (2010) 245-251.
17
18
19
20
21 [10] Y. Zhu, P. Chandra, Y. Shim, Ultrasensitive and selective electrochemical diagnosis of breast
22 cancer based on a hydrazine-Au nanoparticle-aptamer bioconjugate, *Anal. Chem.* 85 (2013) 1058-1064.
23
24
25
26
27 [11] J. Wang, Electrochemical biosensors: Towards point-of-care cancer diagnostics, *Biosens.*
28 *Bioelectron.* 21 (2006) 1887-1892.
29
30
31
32
33 [12] K.J. Huang, J. Li, Y.Y. Wu, Y.M. Liu, Amperometric immunobiosensor for fetoprotein using Au
34 nanoparticles/chitosan/TiO₂/graphene composite based platform, *Bioelectrochem.* 90, (2013) 1623.
35
36
37
38 [13] Sh. Eissa, L. L'Hocine, M. Siaj, M. Zourob, A graphene-based label-free voltammetric
39 immunosensor for sensitive detection of the egg allergen ovalbumin, *Analyst* 138 (2013) 4378-4384.
40
41
42
43
44
45 [14] C. Liu, Q. Jia, C. Yang, R. Qiao, L. Jing, L. Wang, C. Xu, M. Gao, Lateral flow
46 immunochromatographic assay for sensitive pesticide detection by using Fe₃O₄ nanoparticle aggregates
47 as color reagents, *Anal. Chem.* 83 (2011) 6678-6684.
48
49
50
51
52
53
54
55
56
57
58
59
60

- 1
2
3 [15] Y. Zhuo, P.X. Yuan, R. Yuan a, Ya.Q. Chai, C.L. Hong, Bionzyme functionalized-thy
4 composite magnetic nanoparticles for electrochemical immunosensors, Biomaterials 30 (2009) 2284
5
6 2290.
7
8
9
10
11 [16] A.S. Karakoti, S. Das, S. Thevuthasan, S. Seal, PEGylated inorganic nanoparticles, Angewandte
12 Chemie 50 (2011) 1980-1994.
13
14
15
16
17 [17] H. Otsuka Y. Nagasaki K. Kataoka PEGylated nanoparticles for biological and pharmaceutical
18 applications Adv. Drug Deliv. Rev. 64 (2012) 246-255.
19
20
21
22
23 [18] J. Suh K.L Choy, S.K. Lai, J.S. Suk B.C. Tang S. Prabh, J. Hanes PEGylation of nanoparticles
24 improves their cytoplasmic transport. J. Nanomedicine 4 (2007) 735-741.
25
26
27
28
29 [19] I. MartinezMera, M.E. Espinosa, R. Perez Hernandez, J. ArenasAlatorre, Synthesis of magnetite
30 (Fe₃O₄) nanoparticles without surfactants at room temperature, J. Mater.Lett. 61 (2007) 444-4451.
31
32
33
34
35 [20] C.M. Niemeyer, Bioconjugation protocols. New Jersey: Humana; 2004.
36
37
38
39
40 [21] C.W. Scales A.J. Convertine C.L. McCormick Fluorescent labeling of RAFT-generated poly(N
41 isopropylacrylamide) via a facile Maleimide-thiol coupling reaction, Biomacromolecules 7 (2006)
42 1389-1392.
43
44
45
46
47 [22] L. Loo, J.A. Capobianco W. Wu, X. Gao W.Y. Shih, W.H Shih, K. Pourrezaei M.K.
48 Robinson, G.P. Adams Highly sensitive detection of HER2 extracellular domain (ECD) in the
49 serum of breast cancer patients by piezoelectric microcantilevers (PEMFC), Chem. 83 (2011)
50 3392-3397.
51
52
53
54
55
56
57
58
59
60

1
2
3 [23] J.T. Gohringa, P.S. Daleb, X. Fan, Detection of HER2 breast cancer biomarker using the dip
4 ring resonator biosensor, Sens. Actuat. B 146 (2010) 2306
5
6
7

8
9
10 [24] Q.A.M. Al-Khafaji, M. Harris, S. Tombelli, S. Laschi, A.P.F. Turner, M. Mascini, G. Mera, An
11 Electrochemical Immunoassay for HER2 Detection, Electroanalysis 24 (2012) 7435
12
13
14
15
16
17
18
19
20
21
22
23
24
25
26
27
28
29
30
31
32
33
34
35
36
37
38
39
40
41
42
43
44
45
46
47
48
49
50
51
52
53
54
55
56
57
58
59
60